

## Article

# Pyrolysis of Biomass Wastes into Carbon Materials

Małgorzata Sieradzka <sup>1</sup>, Cezary Kirczuk <sup>1</sup>, Izabela Kalemba-Rec <sup>1</sup>, Agata Mlonka-Mędrala <sup>2</sup>  
and Aneta Magdziarz <sup>1,\*</sup>

<sup>1</sup> Faculty of Metals Engineering and Industrial Computer Science, AGH University of Science and Technology, Al. Mickiewicza 30, 30-059 Cracow, Poland; msieradz@agh.edu.pl (M.S.); c.kirczuk@agh.edu.pl (C.K.); kalemba@agh.edu.pl (I.K.-R.)

<sup>2</sup> Faculty of Energy and Fuels, AGH University of Science and Technology, Al. Mickiewicza 30, 30-059 Cracow, Poland; amlonka@agh.edu.pl

\* Correspondence: amagdzia@agh.edu.pl

**Abstract:** This study presents the results of the biomass pyrolysis process focusing on biochar production and its potential energetic (as solid fuel) and material (as adsorbent) applications. Three kinds of biomass waste were investigated: wheat straw, spent coffee grounds, and brewery grains. The pyrolysis process was carried out under nitrogen atmosphere at 400 and 500 °C (residence time of 20 min). A significant increase in the carbon content was observed in the biochars, e.g., from 45% to 73% (at 400 °C) and 77% (at 500 °C) for spent coffee grounds. In addition, the structure and morphology were investigated using scanning electron microscopy. Thermal properties were studied using a simultaneous thermal analysis under an oxidising atmosphere. The chemical activation was completed using KOH. The sorption properties of the obtained biochars were tested using chromium ion (Cr<sup>3+</sup>) adsorption from liquid solution. The specific surface area and average pore diameter of each sample were determined using the BET method. Finally, it was found that selected biochars can be applied as adsorbent or a fuel. In detail, brewery grains-activated carbon had the highest surface area, wheat straw-activated carbon adsorbed the highest amount of Cr<sup>3+</sup>, and wheat straw chars presented the best combustion properties.

**Keywords:** agriculture biomass waste; pyrolysis; biochar; active carbon



**Citation:** Sieradzka, M.; Kirczuk, C.; Kalemba-Rec, I.; Mlonka-Mędrala, A.; Magdziarz, A. Pyrolysis of Biomass Wastes into Carbon Materials. *Energies* **2022**, *15*, 1941. <https://doi.org/10.3390/en15051941>

Academic Editors:

Emmanuel Revellame,  
Randy Maglinao and Alok  
Kumar Patel

Received: 28 January 2022

Accepted: 5 March 2022

Published: 7 March 2022

**Publisher's Note:** MDPI stays neutral with regard to jurisdictional claims in published maps and institutional affiliations.



**Copyright:** © 2022 by the authors. Licensee MDPI, Basel, Switzerland. This article is an open access article distributed under the terms and conditions of the Creative Commons Attribution (CC BY) license (<https://creativecommons.org/licenses/by/4.0/>).

## 1. Introduction

During the 22 and 23 April 2021, leaders of 40 countries attended the Leaders Summit on Climate held by President of United States of America. One of the key points of the meeting was bringing the United States back into the Paris Agreement. A new climate target was established to reduce greenhouse gas emissions by the United States in 2030 by 50–52% compared to the emission level in 2005. The European Union announced that net greenhouse gas emissions will be reduced by at least 55% by 2030, leading to the achievement of a net zero target by 2050. The USA is planning to achieve new climate goals by reducing industry carbon pollution by promoting carbon capture and supporting the use of renewable energy and waste conversion to power industrial facilities [1]. The world environmental policy brings us to the point where the renewable energy source (RES) requires further studies and support for the development of new technologies. This creates a great opportunity to connect the reuse of waste, such as RES, into new energy forms, as well as feedstock applications for other industrial sectors.

Biomass is one of the renewable energy sources with very high potential for energy applications. Solid biomass—mainly forestry and wood and agricultural residues—covers more than two-thirds of the biomass market in Europe. According to Article 3 of the EU Directive “Binding overall Union target for 2030”, the EU member states have endorsed the achievement of a binding minimum 32% share of renewable energy consumption. Biomass can be classified taking into account its origin; therefore, the most important

are woody biomass, agriculture biomass, sewage sludge, and organic waste from the food industry [2]. Wood and agricultural biomass are often called lignocellulosic biomass because they consist of structural components of hemicellulose, cellulose, and lignin [3]. Depending on the type of biomass, the content of these components is different and has a strong impact on their further conversion.

Biomass wastes characterise a wide range of physical and chemical properties, which is why it is difficult to indicate one thermal method for their conversion. Furthermore, the heterogeneity and the predominantly high moisture content of biomass limit its direct application to the energy sector as a fuel [4]. For the valorisation of lignocellulosic feedstocks, a variety of thermochemical methods are needed. Processes such as torrefaction [5], hydrothermal carbonisation [6], pyrolysis [7,8], and gasification are applied depending on the properties of the biomass and the application of the products obtained [9]. There are many studies concerning the thermal process mentioned with respect to different experimental conditions such as temperature, residence time, particle size of materials, type of reactor, presence of catalyst, etc. One of the most interesting investigations is solar pyrolysis [10], catalyst applications [11,12], and subcritical and supercritical water gasification [13]. The management of biomass waste using the pyrolysis process has been widely studied by Poskart et al. [14].

In Poland, annual solid biomass resources have been estimated at approximately 30 million tons, of which 26.7% is agricultural biomass [15], mainly straw (a crop residue). The chemical energy of 1 kg of straw (15% of the moisture content) gives 14.3 MJ heat. Straw characterises low sulphur content, low ash content compared to coal, and high volatile matter [16,17]. Organic waste from the food industry also plays an essential role. Spent coffee grounds (SCG) are being generated around the world because coffee is a very popular beverage. It affects the high amount of spent coffee grounds production every day. It was provided that the spent coffee grounds are rich in fatty acids, amino acids, lignin, polysaccharides, polyphenols, tannins, and flavonoids, thus making this feedstock a potential substrate for biofuel production, adsorbents, and chemical production [18–20]. There are some examples of investigations on the treatment and application of spent coffee grounds: (i) valorisation of SCG in solid biomass fuel in the form of briquettes using xanthan gum under low temperature and low pressure conditions [21]; (ii) gasification of SCG which gave good results and demonstrated the high energy potential of this material [22]; (iii) polyhydroxyalkanoates (chemical industry) [23]. The brewery industry generates spent grains, which are 85% of the total waste generated by brewery. Brewery grains are lignocellulosic feedstock with high protein and nutritive values, and they consist of cellulose (16–25%), protein (15–24%), and lignin (11–27%) [24], which means that they contain components of high added value. Investigations have been carried out for the application of brewery grains in the food industry, energy production, and biotechnological processes [25], because they include bioactive compounds that can extract a wide range of chemicals, for example: polyphenols, lactic, and succinic acids [26,27].

The proper thermal treatment of biomass waste enables the acquisition of a new valuable material such as highly porous activated carbon. Activated carbons might be obtained through several thermochemical and chemical processes. The first step is high-temperature carbonisation, but after that process, the obtained product does not have a developed porous structure. Therefore, its activation is carried out through physical processes, such as high-temperature gasification or chemical treatment using hydroxides. Activated carbon is a common adsorber used in many industries; it is used very frequently in water treatment facilities [28]. One of the most difficult heavy metals to remove from wastewater is chromium [29]. It is also one of the most dangerous contaminants in water, released from various industries such as textiles, metallurgy, electroplating, and others [30]. In the EU, the maximum values of Cr (IV) and Cr (IV) + Cr (III) released into the aquatic environment are 1 and 5 mg/L, respectively [31]. Although trivalent chromium is necessary for living organisms in microamounts, at higher concentrations, it might be lethal [32].

Therefore, the problem of chromium capture from aquatic solutions is a crucial problem that needs to be solved.

Taking into account environmental protection and climate policy, the scientific focus of the authors on the area of enhancing the energetic properties and production of new value-added materials from various types of biomass is fully justified. The presented topic concerns current issues of renewable fuels applications and is very important from the cognitive and practical point of view. The objective of the presented work was to obtain biochars from biomass wastes under pyrolysis and further investigate their properties toward their further application as a solid fuel or adsorbent. It should be emphasised that the utilisation of waste biomass as a fuel or in activated carbon production is a part of a circular economy concept, leading to the minimisation of waste generation and the preservation of natural resources. The concept of circular economy includes treatment, energy production, and waste utilisation. It reflects the assumption of 'zero waste for the EU'. The bioeconomy is crucial for agriculture, food, pharmacy, and energy industries.

## 2. Materials and Methods

In this study, three types of biomass were selected for analysis of their energy and material potential. The following feedstocks were obtained from agricultural and agro-industrial wastes: wheat straw (WS), spent coffee grounds (SCG), and brewery grains (BG). The potential and production of wheat straw in Poland is among the highest among agricultural residues. The spent coffee grounds were collected from the restaurant, while the beer grains came from a brewery located in Poland. The chosen residues are valuable materials that require management, leading to the attainment of ecological and economic benefits.

The studied feedstocks were treated under a pyrolysis process to obtain biochars. Pyrolysis was performed using a laboratory setup with an electrically heated furnace with a horizontal quartz reactor. The laboratory setup scheme is presented in Figure 1. The pyrolysis was carried out under nitrogen atmosphere with a flow rate of 100 mL/min at a temperature of 400 and 500 °C. A c.a. 10 g sample was used. Nitrogen was passed through the reactor system to remove oxygen and obtain a non-oxidised reaction atmosphere. The heating rate of a furnace was 100 °C·min<sup>-1</sup>. The residence time of a sample in process was 20 min. After this, the furnace was cooled, and the obtained biochar was removed. The biochars were named approximately: WS\_400, WS\_500, SCG\_400, SCG\_500, BG\_400, and BG\_500.

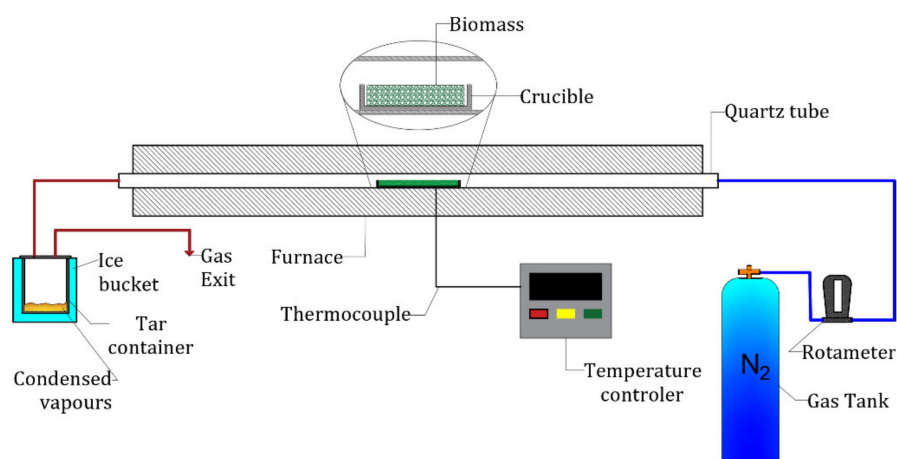


**Figure 1.** Laboratory setup scheme.

The physical and chemical properties of raw materials and biochars were investigated. Moisture (M), ash (A), and volatile matter (VM) contents were performed according to standards (PN-EN ISO 18134-2:2017-03; PN-EN ISO 18122:2016-01; PN-EN ISO 18123:2016-01, respectively). The elemental analyser Leco CHN628 was used to determine the carbon

(C), hydrogen (H), and nitrogen (N) content in the studied samples according to PN-EN ISO 16948:2015-07.

Simultaneous thermal analysis (STA) was carried out to investigate the thermal behaviour of feedstocks and biochars under combustion conditions. During thermogravimetric analysis, TG and DSC curves were collected. The TG curve reflects the mass change of studied material ( $m = f(T)$ ), whereas DSC shows thermal effects (exothermic or endothermic). Additionally, the first derivative of the TG curves was calculated to obtain a DTG curve (Differential Thermogravimetry— $dm/dT = f(T)$ ). The sample was placed in an alumina crucible, and a sample (c.a. 5 mg mass) was heated from ambient temperature to 700 °C at a heating rate of 10 °C/min under air atmosphere with 50 mL min<sup>-1</sup>.

The morphology and structure were studied using scanning electron microscopy with energy-dispersive X-ray spectroscopy (SEM-EDS) (Inspect S50, FEI, Thermo Fischer Scientific, Waltham, MA, USA apparatus). Samples of raw materials and biochars were mounted on metal stubs by double-sided carbon adhesive discs. SEM images were acquired using the secondary electron (SE) detector in the high-vacuum mode. The applied acceleration voltage was 3 keV. Additionally, for the raw and after chromium adsorption samples, the microanalysis of the chemical composition was performed using energy-dispersive X-ray spectroscopy (EDS). The specific surface area of raw and biochar samples was determined using the Brunauer–Emmett–Teller (BET) method using the Quantachrome Poremaster 60 analyzer (Anton Paar, Graz, Austria).

Biochar adsorption experiments were performed using chromium nitrate (Cr(NO<sub>3</sub>)<sub>3</sub>). In each procedure, respectively, 0.2 g of each biochar was placed in chromium solution in an Erlenmeyer flask (250 mL). The pH was constant and equalled 5.00. The chromium solution with biochar was maintained for 24 h using a magnetic stirrer. After the experiments, the solution was analysed, taking into account Cr<sup>3+</sup> concentration using atomic absorption spectrometry (spectrometer of AA Perkin Elmer, Polska, Cracow, Model 3110,  $\lambda = 357.9$  nm). The dried biochar was analysed to study changes in the biochar matrix using SEM-EDS.

The biochar activation was completed using a chemical process with KOH as the activation agent. The reaction parameters were as follows: activation temperature 800 °C, activation time 1 h, nitrogen atmosphere, and mass ratio of biochar to KOH 3:1. After the activation, activated chars were cleaned in HCl to remove KOH, and the next obtained activated carbons were dried and investigated toward its absorption properties.

### 3. Results and Discussion

#### 3.1. Solid Fuel Properties

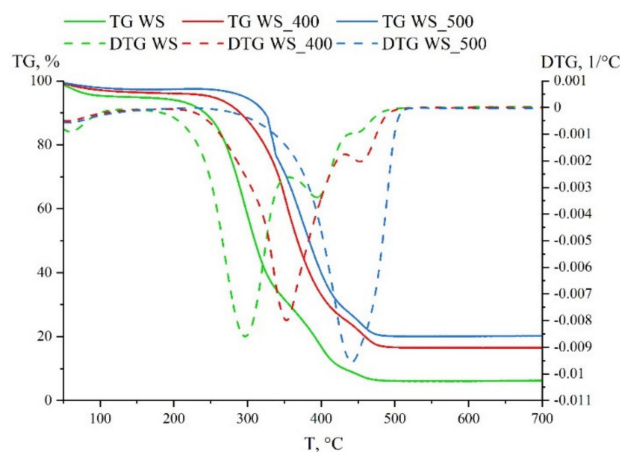
Table 1 presents the proximate and ultimate analysis of the feedstock and biochars obtained at 400 and 500 °C pyrolysis process. All biomass wastes are characterised by different physical properties and elemental composition. The moisture values reflected the condition of the sample used for pyrolysis. It should be noticed that originally spent coffee grounds and brewery grains had very high moisture content (up to 50%). The highest ash content and consequently the lowest volatile matter had wheat straw. SCG and BG had characterised higher volatile matter and lower ash content.

Analysing the elemental composition of samples, BG (brewery grains) had the highest carbon and hydrogen contents among studied wastes. It should be emphasised that WS (wheat straw) and SCG (spent coffee grounds) also had adequate properties for the pyrolysis process to obtain valuable biochars, which can be applied as active carbon or adsorbent for heavy metals. Table 1 presents the changes in elemental composition of raw and biochar samples and reveals that pyrolysis at 400 and 500 °C had an evident effect on the carbon content increase. The most significant increase in carbon content was observed for spent coffee grounds. For BG and WS, the carbonisation effect was observed, too. It can be seen that the increase in pyrolysis temperature did not affect the carbon content in a spectacular way. Thus, it suggests that 400 °C is a sufficient process temperature to obtain biochar with valuable energetic properties.

**Table 1.** Proximate and ultimate analysis of studied feedstock and biochars, wt. % (M—moisture, A—ash, VM—volatile matter, C—carbon, H—hydrogen, and N—nitrogen contents).

Sample	M	A	VM	C	H	N
WS	5.8	6.8	76.0	43.23	5.97	0.97
WS_400		18.2	30.6	62.58	3.95	1.64
WS_500				67.66	2.99	1.74
SCG	14.8	4.0	81.7	44.97	7.47	2.18
SCG_400		8.6	38.4	73.32	5.17	4.17
SCG_500				76.78	3.38	4.25
BG	1.5	2.1	80.3	48.80	6.87	4.39
BG_400		6.2	37.1	69.88	4.87	6.82
BG_500				70.86	3.26	6.80

To study the thermal behaviour under combustion conditions of biochars compared to the raw material, the thermal analysis was carried out. Figures 2–4 present the TG (thermogravimetry—weight loss of sample to initial mass) and DTG (differential thermogravimetry) curves allowing to determine the characteristic temperature of combustion. When the TGA results were compared among the feedstock studied, differences in thermal behaviour were observed. They were probably indicated with the structural composition (hemicellulose, cellulose, and lignin contents) of the raw biomasses. It is confirmed in the intensity and temperature of the DTG peaks. It should be emphasised that besides the mentioned components, biomass wastes contain mineral matter, lipids, and proteins. The wheat straw and brewery grains are lignocellulosic materials but with different content of structural components. Wheat straw was composed of 24% cellulose, 32% hemicellulose and 13% lignin, and brewery waste was composed of 17%, 34%, and 3%, respectively. For WS, two evident peaks were detected at 300 and 397 °C, and one small peak was detected at 451 °C (Figure 2). In the case of SCG and BG, two main DTG peaks were observed at c.a. 300 and c.a. 500 °C. Based on TG and DTG, it can be stated that SCG and BG have a similar fibre composition. Analysing the combustion process of raw WS and biochars, the first stage connected with hemicellulose decomposition was not observed for WS\_400 and WS\_500. For WS\_500 biochar, only one peak of DTG was detected. The TG curves for biochars were shifted toward higher temperature such as for coal, confirming that the carbonisation of this feedstock had an effect and changed the structural properties (ratio of structural constituents). The solid residue at the end of the process had increased from raw WS to WS\_500. A similar trend was observed for brewery grains, but the decomposition temperatures were higher than for WS samples, and the solid residues were lower (Figure 4). In biochars BG\_400 and BG\_500, the peak reflected to hemicellulose was not observed, either. In the case for SCG samples that different thermal effects were observed.

**Figure 2.** Thermal behaviour (TG and DTG curves) of wheat straw (WS) and biochars (WS\_400 and WS\_500) in an air atmosphere (combustion conditions).

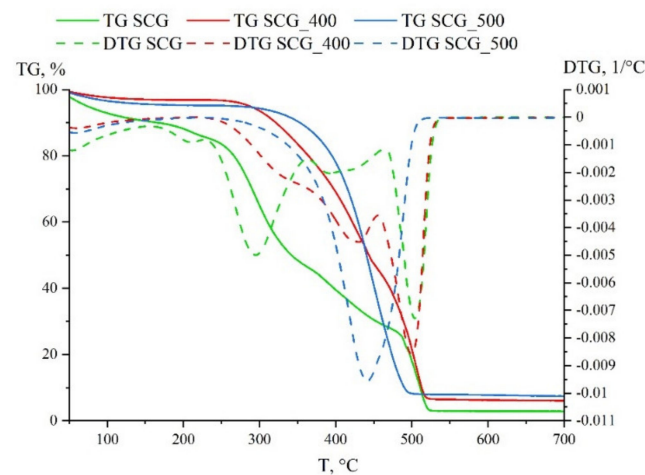


**Figure 3.** Thermal behaviour (TG and DTG curves) of spent coffee grounds (SCG) and biochars (SCG\_400 and SCG\_500) in air atmosphere (combustion conditions).

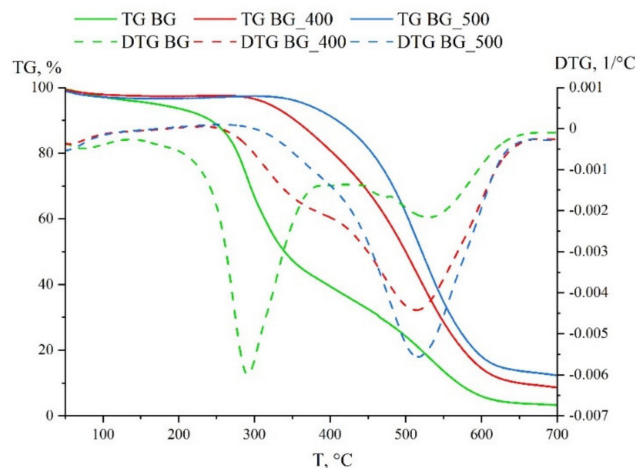


**Figure 4.** Thermal behaviour (TG and DTG curves) of brewery grains (BG) and biochars (BG\_400 and BG\_500) under air atmosphere (combustion conditions).

The results of the thermogravimetric analysis provided data to calculate the key combustion parameters. The following parameters were defined based on the TG and DTG curves: ignition temperature, burnout temperature, temperature of the highest peak DTG, maximum and average mass loss rate, as well as times of maximum peak, ignition, burnout, and  $DTG/DTG_{max}$  range = 0.5 ( $\Delta t_{1/2}$ ). These parameters were used to calculate the following indexes: ignition ( $D_i$ ), burnout ( $D_f$ ), and combustion ( $S$  and  $H_f$ ) [33]. The methodology of calculating indexes and establishing parameters is described in papers [34–36]. The results of the calculations are presented in Table 2. The fuel properties of ignition, combustion, and burnout are reflected in the combustibility index  $S$ . The highest values were obtained for Straw 500 °C at level  $5.80 \times 10^{-7}$ . The general tendency for studied materials as well as the literature review shows that a higher value of the  $S$  index is obtained for raw materials than for biochars. This is caused by the high amount of VM in the sample. In case of WS\_500, the high value of the  $S$  index is affected by the highest maximum mass loss rate. The maximum mass loss rate parameter for WS\_500 was 21.7 wt.%/min; in comparison, the same parameter for SCG\_500 was equal to 11.5 wt.%/min. The combustion process of WS\_500 was very dynamic, which can also be noted on the DTG curve (Figure 1). Additionally, the result of the  $S$  index is confirmed by the  $D_i$  index tendency. The high value of  $D_i$  proves to release a high amount of volatile matter during the combustion process, which confirms that combustion starts at an early stage for this fuel. The rate and intensity

of the combustion process is reflected in the  $H_f$  index. The lowest value was calculated for the BSG sample and obtained a level of 816. The lower the value of  $H_f$ , the better the combustion properties of the fuel. For comparison, in the case of coal, this index is around 2000 [37].

**Table 2.** Combustion parameters of studied feedstock and biochars.

Sample	Di, wt. %/min <sup>3</sup>	Df, wt. %/min <sup>4</sup>	S, min <sup>-2</sup> °C <sup>-3</sup>	Hf, °C
WS	0.0149	$3.52 \times 10^{-4}$	$4.70 \times 10^{-7}$	834
WS_400	0.0105	$2.15 \times 10^{-4}$	$2.66 \times 10^{-7}$	1111
WS_500	0.0246	$5.80 \times 10^{-4}$	$5.82 \times 10^{-7}$	1055
SCG	0.0078	$1.47 \times 10^{-4}$	$3.60 \times 10^{-7}$	1438
SCG_400	0.0072	$1.06 \times 10^{-4}$	$2.59 \times 10^{-7}$	1687
SCG_500	0.0077	$1.61 \times 10^{-4}$	$2.12 \times 10^{-7}$	1447
BG	0.0115	$1.67 \times 10^{-4}$	$2.54 \times 10^{-7}$	816
BG_400	0.0027	$0.482 \times 10^{-4}$	$0.72 \times 10^{-7}$	1661
BG_500	0.0033	$0.554 \times 10^{-4}$	$0.77 \times 10^{-7}$	1756

To study the morphological and structural changes, scanning electron microscopy analysis was performed. Figures 5–7 present SEM images of spent coffee grounds, brewery grains, and wheat straw. The shape and size of the raw spent coffee grounds and raw brewery grains are similar and different from the raw wheat straw particles. The raw wheat straw particles are much finer. However, all raw samples were characterised by a dense structure. After pyrolysis processes, the pores were created, especially in the spent coffee grounds and brewery grains. Independently from process temperature, the entire surface of biochars from spent coffee and brewery grains was covered with pores. The pore diameter was up to 50  $\mu\text{m}$ . In the case of biochars from wheat straw, a small amount of pores was observed on the surface. Their amount was increased with increasing the process temperature, but the pores were very small. The SEM images of the all obtained activated carbons show more porous structures. For all samples, the structure was crashed, but the micropores are visible. The structure of spent coffee grounds partially consists of pores with inside micropores. The micropores in the activated carbons surface were also observed by other researchers [38,39].

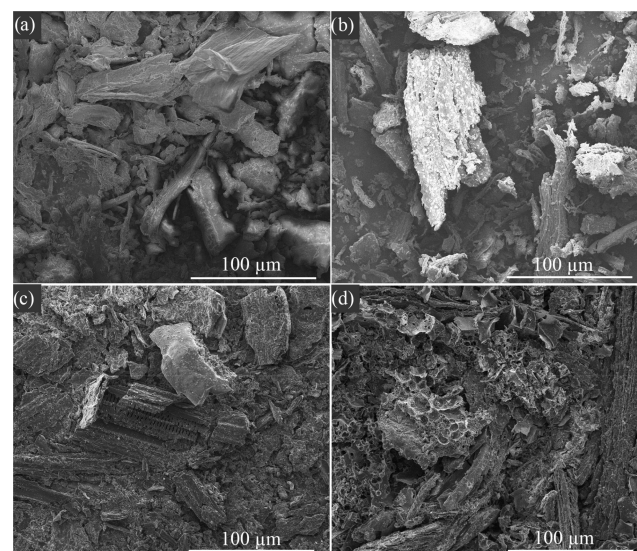


**Figure 5.** SEM images of the wheat straw (WS) (a) raw, (b) WS\_400, (c) WS\_500, (d) after activation.

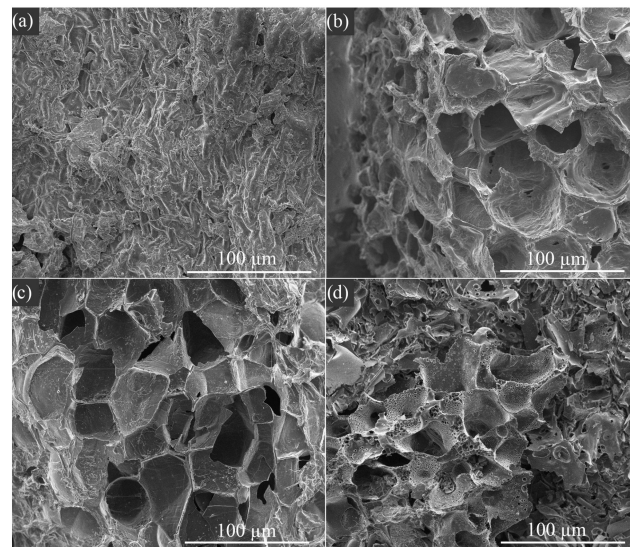


**Figure 6.** SEM images of the spent coffee grounds (SCG) (a) raw, (b) SCG\_400, (c) SCG\_500, (d) after activation.

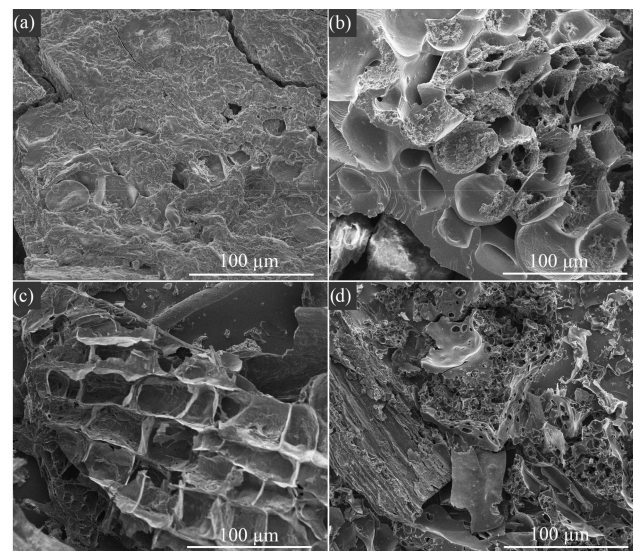


**Figure 7.** SEM images of the brewery grains (BG) (a) raw, (b) BG\_400, (c) BG\_500, (d) after activation.

### 3.2. Adsorbent Properties

Table 3 presents the results for the specific surface area (BET) of raw biomass and biochars. All samples had characterised a very low specific area. A significant increase in surface after the pyrolysis process in biochars was not observed, even the decrease for WS\_500 and BG\_500. The high amount of ash in biochars and the condensed volatile matter from the hemicellulose decomposition could influence the limitation in the development of a specific surface area. In the case of SCG, it was not possible to measure the BET surface area. It was assumed that the samples were not porous, only that they had a geometric surface reflected in the external surface of the particle.

**Table 3.** Specific surface area (BET) of studied feedstock and biochars (obtained after the pyrolysis).

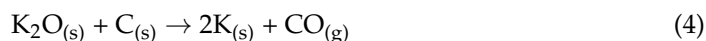
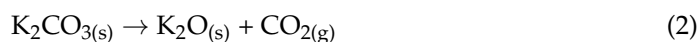
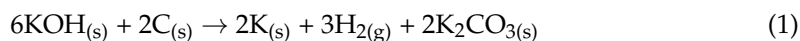
Specific surface area (BET), m <sup>2</sup> /g	WS	WS_400	WS_500	SCG	BG	BG_400	BG_500
	2.25	2.68	1.82	0.06	0.36	0.67	0.27

For materials application examination, products received at 400 °C were selected for active carbon production and further adsorption of chromium testing. The porosity of the obtained active carbons by KOH chemical activation of biochars was noticeably increased. This effect was confirmed according to the data from the literature, indicating that KOH activation leads to microporous carbon-rich material production with a highly developed specific area and higher pore volume (see Table 4 and Figures 5, 6 and 7d) [40].

**Table 4.** Specific surface area (BET) biochars obtained at 400 °C pyrolysis after activation process.

Specific surface area (BET), m <sup>2</sup> /g	WS_400	SCG_400	BG_400
	1939.54	2510.06	2618.60

The highest specific surface area was noted for active carbon obtained from brewery grains char (400 °C). The development of the porous structure and surface area of all biochars using KOH chemical activation is the effect of the following reactions [36]:



As it was confirmed, biochars obtained with lower ash content are good material for the production of active carbon. The high ash content in biochar can have a positive influence on fertiliser application and sorption properties, especially for heavy metal removal. The adsorption properties of biochars were studied on the basis of chromium ion adsorption. It is very important to control the concentration of Cr (III) in potable water. For this study, the solution of 22 mg/L Cr (III) content was analysed as a reference. After the process, biochars and chromium solutions were analysed. The EDS analysis (Figure 8) shows that chromium was absorbed by biochars: 2.5 wt. % in the spent coffee grounds, 1.1 wt. % in the brewery grains, and 2.6 wt. % in the wheat straw were found. Additionally, chemical analysis of the chromium solution had confirmed the decrease of the chromium content in the studied solutions from 22 to 0.10 mg/L for WS, 14 mg/L for SCG, and 15.01 mg/L for BG.

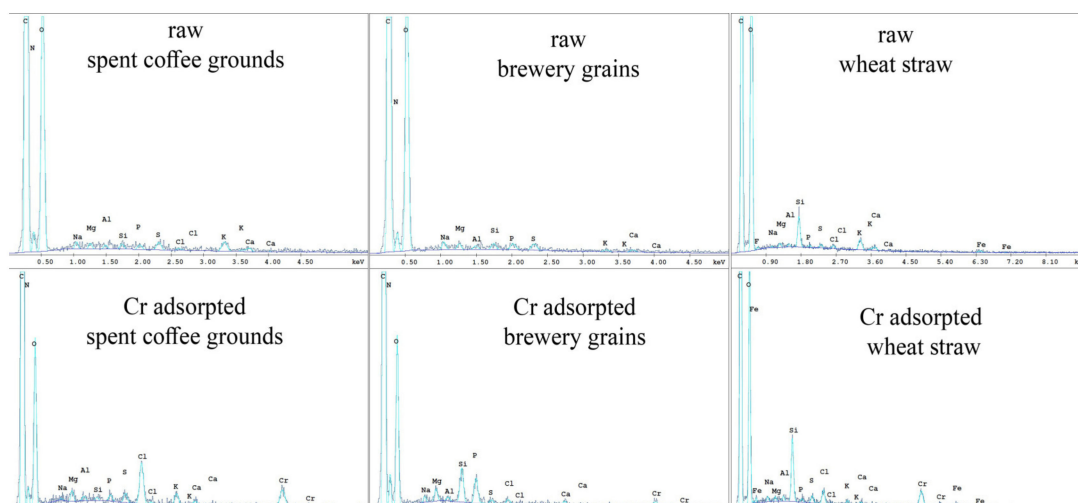


**Figure 8.** EDS spectra for biochars obtained at 400 °C and after the chromium adsorption.

#### 4. Conclusions

Biochars obtained by the low-temperature pyrolysis of lignocellulosic biomass wastes can have a very wide range of applications. Depending on their physical and chemical properties, they can be utilised in the energy sector, as a substrate for active carbon production, and finally as a sorbent for pollutants. The obtained biochars had a significant increase in carbon content (up to c.a. 70% of C) and lower O/C ratio. Thermal analysis confirmed the decomposition of hemicellulose in studied biomass wastes during pyrolysis. The combustion of all obtained biochars proceeded at temperatures higher than those of the raw materials. Obtained biochars were carbon-enriched material; however, the fuel properties were enhanced mostly in the case of spent coffee grounds, which are characterised by the highest initial volatile matter content. Therefore, materials characterised by high volatile matter content are the most suitable feedstock for thermal pretreatment and the production of carbon-rich fuel.

The chemical activation process went successfully, giving materials with specific surface area c.a. 2500 m<sup>2</sup>/g for biochars of brewery grains and spent coffee grounds even with low ash content in raw materials. The activation properties were confirmed during the adsorption of the Cr (III) ion. Therefore, only WS activated biochar fulfils the EU limits determined for chromium capture in water. It might be associated with a presence of functional groups in the biochar, which effectively participate in the adsorption of heavy metals from water solutions. The presented results present possibilities and give the knowledge for further investigations of biomass utilisation with added value to the environment.

In conclusion, it can be verified that the application of the obtained biochars depends on its physicochemical properties such as surface area, pore size and volume, catalytic activity, adsorption efficiency, and chemical composition (carbon and ash contents). Moreover, it can be stated that biochar is one of the most desirable products of biomass wastes obtained under thermal conversion. It has numerous applications and benefits in many fields: the energy sector (carbon replacement, carbon sequestration), environmental protection (adsorbent for pollutants), the agriculture sector (fertiliser), and others. Finally, these actions influence climate change mitigation and environmental management (reduction in waste disposal).

**Author Contributions:** A.M.: project administration, funding acquisition, conceptualisation, methodology, writing the original draft, data curation, and investigation. C.K.: writing, editing, and investigation. M.S.: investigation, review, writing, and visualisation. I.K.-R.: writing, editing, and investigation. A.M.-M.: data curation, investigation, writing, review, and editing. All authors have read and agreed to the published version of the manuscript.

**Funding:** This work has received funding from the European Union's Horizon 2020 Research and Innovation Programme under the Marie Skłodowska-Curie grant agreement no 823745.

**Institutional Review Board Statement:** Not applicable.

**Informed Consent Statement:** Not applicable.

**Conflicts of Interest:** The authors declare no conflict of interest.

#### References

1. Leaders Summit on Climate. Available online: <https://www.state.gov/leaders-summit-on-climate/> (accessed on 18 January 2022).
2. Vassilev, S.V.; Vassileva, C.G.; Vassilev, V.S. Advantages and disadvantages of composition and properties of biomass in comparison with coal: An overview. *Fuel* **2015**, *158*, 330–350. [CrossRef]
3. Nimmanterdwong, P.; Chalermsoinuwan, B.; Piumsomboon, P. Prediction of lignocellulosic biomass structural components from ultimate/proximate analysis. *Energy* **2021**, *222*, 119945. [CrossRef]
4. Roman, K.; Roman, M.; Szadkowska, D.; Szadkowski, J.; Grzegorzewska, E. Evaluation of physical and chemical parameters according to energetic willow (*Salix viminalis* L.) cultivation. *Energies* **2021**, *14*, 2968. [CrossRef]
5. Szwaja, S.; Magdziarz, A.; Zajemska, M.; Poskart, A. A torrefaction of *Sida hermaphrodita* to improve fuel properties. Advanced analysis of torrefied products. *Energ. Renew.* **2019**, *141*, 894–902. [CrossRef]

6. Czerwińska, K.; Śliz, M.; Wilk, M. Hydrothermal carbonization process: Fundamentals, main parameter characteristics and possible applications including an effective method of SARS-CoV-2 mitigation in sewage sludge: A review. *Renew. Sustain. Energy Rev.* **2022**, *154*, 111873. [CrossRef]
7. Mlonka-Mędrala, A.; Evangelopoulos, P.; Sieradzka, M.; Zajemska, M.; Magdziarz, A. Pyrolysis of agriculture waste biomass towards gas fuel and high-quality char production-experimental and numerical investigations. *Fuel* **2021**, *296*, 120611. [CrossRef]
8. Roman, K.; Barwicki, J.; Hryniewicz, M.; Szadkowska, D.; Szadkowski, J. Production of electricity and heat from biomass wastes using a converted aircraft turbine AI-20. *Processes* **2021**, *9*, 364. [CrossRef]
9. Gao, N.; Li, A.; Quan, C.; Qu, Y.; Mao, L. Characteristics of hydrogen-rich gas production of biomass gasification with porous ceramic reforming. *Int. J. Hydrogen Energy* **2012**, *37*, 9610–9618. [CrossRef]
10. Sobek, S.; Werle, S. Solar pyrolysis of waste biomass: A comparative study of products distribution, in situ heating behavior, and application of model-free kinetic predictions. *Fuel* **2021**, *292*, 120365. [CrossRef]
11. Chai, Y.; Wang, M.; Gao, N.; Duan, Y.; Li, J. Experimental study on pyrolysis/gasification of biomass and plastics for H<sub>2</sub> production under new dual-support catalyst. *Chem. Eng. J.* **2020**, *396*, 125260. [CrossRef]
12. Fernandez, E.; Santamaria, L.; Artetxe, M.; Amutio, M.; Arregi, A.; Lopez, G.; Bilbao, J.; Olazar, M. Conditioning the volatile stream from biomass fast pyrolysis for the attenuation of steam reforming catalyst deactivation. *Fuel* **2022**, *312*, 122910. [CrossRef]
13. Okolie, J.A.; Nanda, S.; Dalai, A.K.; Berruti, F.; Kozinski, J.A. A review on subcritical and supercritical water gasification of biogenic, polymeric and petroleum. *Renew. Sustain. Energy Rev.* **2020**, *119*, 109546. [CrossRef]
14. Poskart, A.; Skrzyniarz, M.; Sajdak, M.; Zajemska, M.; Skibiński, A. Management of lignocellulosic waste towards energy recovery by pyrolysis in the framework of circular economy strategy. *Energies* **2021**, *14*, 5864. [CrossRef]
15. Flanders Investment & Trade in Poznań, Renewable Energy in Poland. 2019. Available online: [https://www.flandersinvestmentandtrade.com/export/sites/trade/files/market\\_studies/2019-Poland-Renewable\\_Energy.pdf](https://www.flandersinvestmentandtrade.com/export/sites/trade/files/market_studies/2019-Poland-Renewable_Energy.pdf) (accessed on 18 January 2022).
16. Li, S.; Song, H.; Hu, J.; Yang, H.; Zou, J.; Zhu, Y.; Tang, Z.; Chen, H. CO<sub>2</sub> gasification of straw biomass and its correlation with the feedstock characteristics. *Fuel* **2021**, *297*, 120780. [CrossRef]
17. Proszak-Miasik, D.; Jarecki, W.; Nowak, K. Selected parameters of oat straw as an alternative energy raw material. *Energies* **2022**, *15*, 331. [CrossRef]
18. Atabani, A.E.; Ala'a, H.; Kumar, G.; Saratale, G.D.; Aslam, M.; Khan, H.A.; Said, Z.; Mahmoud, E. Valorization of spent coffee grounds into biofuels and value-added products: Pathway towards integrated bio-refinery. *Fuel* **2019**, *254*, 115640. [CrossRef]
19. Lee, X.J.; Ong, H.C.; Gao, W.; Ok, Y.S.; Chen, W.-H.; Goh, B.H.H.; Chong, C.T. Solid biofuel production from spent coffee ground wastes: Process optimisation, characterisation and kinetic studies. *Fuel* **2021**, *292*, 120309. [CrossRef]
20. Espuelas, S.; Marcelino, S.; Echeverría, A.M.; del Castillo, J.M.; Seo, A. Low energy spent coffee grounds briquetting with organic binders for biomass fuel manufacturing. *Fuel* **2020**, *278*, 118310. [CrossRef]
21. Seco, A.; Espuelas, S.; Marcelino, S.; Echeverría, A.M.; Prieto, E. Characterization of biomass briquettes from spent coffee grounds and xanthan gum using low pressure and temperature. *Bioenergy Res.* **2020**, *13*, 369–377. [CrossRef]
22. Kibret, H.A.; Kuo, Y.L.; Ke, T.Y.; Tseng, Y.H. Gasification of spent coffee grounds in a semi-fluidized bed reactor using steam and CO<sub>2</sub> gasification medium. *J. Taiwan Inst. Chem. Eng.* **2021**, *119*, 115–127. [CrossRef]
23. Corchado-Lopo, C.; Martínez-Avila, O.; Marti, E.; Llimós, J.; Busquets, A.M.; Kucera, D.; Obruca, S.; Llenas, L.; Ponsá, S. Brewer's spent grain as a no-cost substrate for polyhydroxyalkanoates production: Assessment of pretreatment strategies and different bacterial strains. *N. Biotechnol.* **2021**, *62*, 60–67. [CrossRef]
24. Mishra, P.K.; Gregor, T.; Wimmer, R. Utilising brewer's spent grain as a source of cellulose nanofibres following separation of protein-based biomass. *BioResources* **2017**, *12*, 107–116. [CrossRef]
25. Weiermuller, J.; Akermann, A.; Laudensack, W.; Chodorski, J.; Blank, L.M.; Ulber, R. Brewers' spent grain as carbon source for itaconate production with engineered *Ustilago maydis*. *Bioresour. Technol.* **2021**, *336*, 125262. [CrossRef]
26. Mussatto, S.I.; Dragone, G.; Roberto, I.C. Brewers' spent grain: Generation, characteristics and potential applications. *J. Cereal Sci.* **2006**, *43*, 1–14. [CrossRef]
27. Barbosa-Pereira, L.; Bilbao, A.; Vilches, P.; Angulo, I.; Luis, J.; Fité, B.; Paseiro-Losada, P.; Cruz, J.M. Brewery waste as a potential source of phenolic compounds: Optimisation of the extraction process and evaluation of antioxidant and antimicrobial activities. *Food Chem.* **2014**, *145*, 191–197. [CrossRef]
28. Han, T.; Lu, X.; Sun, Y.; Jiang, J.; Yang, W.; Jönsson, P.G. Magnetic bio-activated carbon production from lignin via a streamlined process and its use in phosphate removal from aqueous solutions. *Sci. Total Environ.* **2020**, *708*, 135069. [CrossRef]
29. Kaźmierczak, B.; Molenda, J.; Swat, M. The Adsorption of chromium (III) ions from water solutions on biocarbons obtained from plant waste. *Environ. Technol. Innov.* **2021**, *23*, 101737. [CrossRef]
30. Bahador, F.; Foroutan, R.; Esmaili, H.; Ramavandi, B. Enhancement of the chromium removal behavior of moringa oleifera activated carbon by chitosan and iron oxide nanoparticles from water. *Carbohydr. Polym.* **2021**, *251*, 117085. [CrossRef] [PubMed]
31. Vaiopoulou, E.; Gikas, P. Regulations for chromium emissions to the aquatic environment in Europe and elsewhere. *Chemosphere* **2020**, *254*, 126876. [CrossRef] [PubMed]
32. Payel, S.; Hashem, M.A.; Hasan, M.A. Recycling Biochar Derived from tannery liming sludge for chromium adsorption in static and dynamic conditions. *Environ. Technol. Innov.* **2021**, *24*, 102010. [CrossRef]
33. Sieradzka, M.; Gao, N.; Quan, C.; Mlonka-Mędrala, A.; Magdziarz, A. Biomass thermochemical conversion via pyrolysis with integrated CO<sub>2</sub> capture. *Energies* **2020**, *13*, 1050. [CrossRef]

34. Parshetti, G.K.; Kent Hoekman, S.; Balasubramanian, R. Chemical, structural and combustion characteristics of carbonaceous products obtained by hydrothermal carbonization of palm empty fruit bunches. *Bioresour. Technol.* **2013**, *135*, 683–689. [[CrossRef](#)]
35. Magdziarz, A.; Mlonka-Mędrala, A.; Sieradzka, M.; Aragon-Briceño, C.; Pożarlik, A.; Bramer, E.A.; Brem, G.; Niedzwiecki, Ł.; Pawlak-Kruczek, H. Multiphase analysis of hydrochars obtained by anaerobic digestion of municipal solid waste organic fraction. *Renew. Energy* **2021**, *17*, 108–118. [[CrossRef](#)]
36. Mureddu, M.; Dessi, F.; Orsini, A.; Ferrara, F.; Pettinau, A. Air- and oxygen-blown characterization of coal and biomass by thermogravimetric analysis. *Fuel* **2018**, *212*, 626–637. [[CrossRef](#)]
37. Cuong, D.V.; Matsagar, B.M.; Lee, M.; Hossain, M.S.A.; Yamauchi, Y.; Vithanage, M.; Sarkar, B.; Ok, Y.S.; Wu, K.C.-W.; Hou, C.-H. Critical review on biochar-based engineered hierarchical porous carbon for capacitive charge storage. *Renew. Sustain. Energy Rev.* **2021**, *145*, 111029. [[CrossRef](#)]
38. Deng, Z.; Sun, S.; Li, H.; Pan, D.; Patil, R.R.; Guo, Z.; Seok, I. Modification of coconut shell-based activated carbon and purification of wastewater. *Adv. Compos. Hybrid Mater.* **2021**, *4*, 65–73. [[CrossRef](#)]
39. Aboua, K.N.; Yobouet, K.Y.A.; Yao, K.B.; Goné, D.L.; Trokourey, A. Investigation of dye adsorption onto activated carbon from the shells of Macoré fruit. *J. Environ. Manag.* **2015**, *156*, 10–14. [[CrossRef](#)]
40. Ding, S.; Liu, Y. Adsorption of CO<sub>2</sub> from flue gas by novel seaweed-based KOH-activated porous biochars. *Fuel* **2020**, *260*, 116382. [[CrossRef](#)]